Geometric Control of a Quadrotor with a Suspended Load

Subtitle

N.N. Vo

June 15, 2017

DCSC

TUDelft

Geometric Control of a Quadrotor with a Suspended Load
Subtitle

Master of Science Thesis

For obtaining the degree of Master of Science in Mechanical Engineering at Delft University of Technology

N.N. Vo

June 15, 2017

Faculty of Mechanical, Maritime and Materials Engineering · Delft University of Technology

Delft University of Technology

Abstract

A Quadrotor is a type of Unmanned Aerial Vehicle that has received an increasing amount of attention recently with many applications including search and rescue, surveillance, supply of food and medicines as disaster relief and object manipulation in construction and transportation.

An interesting control problem is the Load Position Tracking of a cable suspended load. The system is highly nonlinear and under-actuated. The load cannot be actuated directly and has a natural swing at the end of each Quadrotor movement. A Nonlinear Geometric Control approach allows differential geometric techniques to be applied to systems control, which can be defined on a smooth nonlinear configuration space. This creates a coordinate-free dynamic model, while avoiding the problem of singularities on local charts.

****

Intro about GC.. Reasons to consider GC..

****

Where simple linear control methods are restricted to small angle movements, nonlinear control methods allow more aggressive and faster movements. The goal of the project is to investigate the effects on load position tracking performance when the system is modeled and controlled via a Nonlinear Geometric Control approach.

****

The Quadrotor-Load system is modeled in a compact and coordinate-free fashion which allows the inherent geometric properties of the system to be controlled.

The main goal of this thesis is to research the effects on a cable-suspended load transportation using quadrotors, by involving complex or aggressive maneuvering through implementation of Non-Linear Geometric Control. Where linear control methods are restricted to small angle movement, non-linear control methods allow more aggressive movements.

Furthermore, the studied control techniques are explained and their advantages are addressed. Several trajectory generation approaches and the related optimization techniques are studied. Their applications, with different purposes such as obstacle avoidance, time-optimal and swing-free trajectory planning are explained. The survey is concluded with a discussion

about finding a suitable **
Define suitable

****

control design to achieve the quadrotor-assisted task involving manipulation of a cable-suspended load.

****

Acknowledgements

I would like to thank my supervisors dr.ir. T. Keviczky from Delft Center of Systems and Control, and ir. B. van Vliet from Alten Nederland B.V. for their assistance during my research and the writing of this thesis. I would also like to thank all colleagues from Alten and TU Delft for their time and advice whenever this was needed.

Delft, University of Technology   N.N. Vo
June 15, 2017

Table of Contents

List of Figures

List of Tables

Chapter 1

Introduction

A Quadrotor (QR) is a type of Unmanned Aerial Vehicle (UAV) that has received an increasing amount of attention recently with many applications being actively investigated. Possible applications include search and rescue, surveillance, reliable supply of food and medicines as disaster relief and object manipulation in construction and transportation. It has already proven itself useful for many tasks like multi-agent missions, mapping, explorations, transportation and entertainment such as acrobatic performances.

The inspiration for this research is build upon the idea of creating a system of multiple autonomous QRs for a cooperative towing task. The advantage of such a system for object manipulation is the possibility to reduce complexity of the individual robot, decrease cost over traditional robotic systems and high reliability. One can think of examples in nature, where individuals coordinate, cooperate and collaborate to perform tasks that they individually can not accomplish. Redundancy makes development of fail safe control methods possible and can extend the capabilities of a single robot.

****

Bart: suggestion: creating a system of multiple autonomous QRs?
Nam: Zin aangepast.

****

Considering a multi-agent task, one can think of multiple QRs assisting in the transportation of a common load. This cooperation can be executed in many ways, but this research focuses on QRs with a cable-suspended load in motion. The suspended object naturally continues to swing at the end of every movement. In case a residual motion can result in damage or in order to avoid obstacles and path following, an accurate positioning is required. Reducing the oscillation, or controlling the position of the suspended load might be necessary, but is challenging in the fact that this cable-suspended system is under-actuated. Possible objectives are minimizing the oscillations of the load during or after motion, minimizing the time to position the load, trajectory tracking, trajectory generation and obstacle avoidance.

****

Bart: Suggestion place under motivation of research inspiration, this forms a nice bridge.
Nam: Ik heb dit juist naar boven geplaatst. The inspiration ..... single robot.

****

1-1 Aim and Motivation

The aim is to control the position of a suspended load using a QR. Before considering multiple QRs, it is important to investigate the possibilities of a single QR system. Hence, in this research a single QR is considered for the transportation of a cable suspended load, which will exert additional forces and torques on the QR. This is a challenging control problem in the fact that the QR system is under-actuated. Adding a suspended load will add extra DOFs and oscillations of the load occur at the end of every movement.

****

Bart: Suggestion: Since QRs with suspended load are scarcely investigated it is important to investigate a single QR first before the multiple QRs can be considered.
Nam: Zie boven

****

The system can be divided into two subsystems. The first subsystem is where the cable tension is non-zero and the distance between the QR and the load is defined by the cable length. Both QR and load are coupled as one system. The second subsystem is where the cable tension is zero, such that the QR and load in free fall are two separate decoupled systems. This research focuses on the first subsystem, such that the cable tension is non-zero. In order to control both subsystems, hybrid control must be applied, which is considered out of the scope of this research.

Former work on QR attitude- and position control often rely on linear control methods such as PID controller[?], MPC [1] and LQR control [?]. The dynamics are linearized around an equilibrium point, describing the system dynamics by a set of linear differential equations. The control of a QR-Load system is a very specific case, and former work includes MPC [2] and LQR[?] control approaches, where an optimal control strategy is used to minimize the swing of the load.

The reason that linear control near an equilibrium state is commonly applied, is partly to avoid difficulties that come with modeling and controlling the non-linearities of the system. Non-linear control systems are often governed by nonlinear differential equations and are able to represent the dynamics in a more realistic manner. However, linear control limits the system to small angle movements, as the optimization will not allow large angles that deviate to far from the linearized point. For applications that require fast aggressive maneuvers, this type of modeling and control will not be sufficient.

A possible nonlinear control approach is Nonlinear MPC, which is a variant of MPC that uses a nonlinear dynamical system to predict the required inputs. While these problems are convex in linear MPC, in nonlinear MPC they are not convex anymore. This poses challenges for both Nonlinear MPC stability theory and numerical solution.

Nonlinear Geometric Control is a nonlinear model based control technique based on a modeling approach involving the concepts of differential geometry. This results in a globally defined coordinate-free dynamical model, while preventing issues regarding singularities, and enabling the design of controllers that offer almost-global convergence properties.

Former work includes a nonlinear geometric PID controller control of a QR [4] and nonlinear geometric control of the load position, load attitude and QR attitude of a QR-Load system

[5, 6]. Geometric Control for the control of QR systems is used less frequently, despite the advantageous properties of differential geometry.

This motivates to investigate the possibilities and limitations of the less used nonlinear Geometric Control design, and compare this to a commonly used linear control strategy. The question is which advantages or disadvantages this nonlinear approach has compared to a linear approach, in terms of stability and performance.

Different aspects involving the modeling and control for the QR-Load system must be investigated, for it can be expected that the non-linearity will have a great influence in the representation of the dynamics and the stability, accuracy and type of control design.

System consists of two sub-systems Limited to subsystem where the tension of the cable is non-zero.

1-2 Organization of the Report

In this first chapter, a brief introduction of the subject is given and the problem is described. This is followed by discussing the aim, motivation and contributions of this thesis for this research. The organization of the report is as follows.

In Chapter 2 the dynamics of the QR-Load system is described by the laws of kinematics and the application of Newton's laws or Lagrangian mechanics. Opposed to the classical modeling techniques, it is also possible to describe the system's configuration space as a differentiable manifold using the tools of differential geometry. Geometric Mechanics is used to understand and derive the equations of motion of a system in order to allow its analysis and design.

The system dynamics are represented on nonlinear manifolds and this allows nonlinear geometric controllers to be designed on these same manifolds. The control design is presented in Chapter 3. The controller has a cascaded structure, where the different control loops are accountable for different flight modes.

Different tracking objectives can be defined in order to test the performance of both an LQR control design and a nonlinear Geometric Control design. Chapter 4 describes the experiments that are done to investigate the abilities and performance of a nonlinear Geometric Control design. The results and findings are presented and discussed.

In the final chapter a summary of the thesis is given, followed by the conclusions that were made based on the results of the experiments. Finally, recommendations are given which could serve as an starting point for future work.

Chapter 2

Dynamic Model

A mathematical model of the system needs to be derived in order to simulate and study the effects of Geometric Control. The assumptions that are applied to simplify the model are discussed in Section 2-1.

In Section 2-2 an introduction is given about Geometric Mechanics, which is a modern description of the classical mechanics from the perspective of Differential Geometry. Differential Geometry is a discipline in mathematics that studies manifolds and their geometric properties, using the tools of calculus. Geometric Mechanics is used to model the QR-Load system, which is described in Section 2-3.

To derive the equations of motions traditional modeling methods often parameterize the rotations in a local coordinate system. Euler angles are commonly used, however these coordinates might result in singularities. Furthermore, there are 24 possible sets of Euler angles and many different conventions are used, which leads to ambiguity. The definition of Euler angles is not unique and a sequence of rotations is not commutative. Therefore, Euler angles are never expressed in terms of the external frame, or in terms of the co-moving rotated body frame, but in a mixture.

In order to avoid these complexities, the dynamics of the QR-Load system can be globally expressed on the Special Orthogonal Group $SO(3)$, *2-sphere* $\mathbb{S}^2$ and Special Euclidean Group $SE(3)$. This leads to a compact notation of the equations of motion, making the large amount of trigonometric functions unnecessary, that Euler angles normally introduce.

2-1   Modeling Assumptions

The QR model representation is shown in Figure 2-1. Three Cartesian coordinate frames are defined:
- The body-fixed reference frame $\{\mathcal{B}\}$ (Body Frame)

    with unit vectors $\{\mathbf{b}_1, \mathbf{b}_2, \mathbf{b}_3\}$ along the axes

- The ground-fixed reference frame $\{\mathcal{I}\}$ (Inertial Frame)

    with unit vectors $\{\mathbf{e}_1, \mathbf{e}_2, \mathbf{e}_3\}$ along the axes

- The intermediary frame $\{\mathcal{C}\}$, ($\{\mathcal{I}\}$ rotated by the yaw angle ψ)

    with unit vectors $\{\mathbf{c}_1, \mathbf{c}_2, \mathbf{c}_3\}$ along the axes

Figure 2-1: Quadrotor model representation

Figure 2-2: Quadrotor with Load model representation

The position of the body frame is described by a vector evolving on $\mathbb{R}^3$, and is represented with respect to the inertial frame. The orientation, also called attitude, of the body frame with respect to the inertial frame evolves on a nonlinear space, for which several methods exist to describe this, such as *Euler Angles*, quaternions or rotation matrices.

The complex dynamics of the rotors and their interactions with drag and thrust forces are represented by a simplified model. The angular speed ω_i of rotor i, for $i = 1, \ldots, 4$, generates a force F_i parallel to the direction of the rotor axis of rotor i, given by

$$F_i = \left(\frac{K_v K_\tau \sqrt{2\rho A}}{K_t} \omega_i \right)^2 = b\omega_i^2 \tag{2-1}$$

where K_v, K_t are constants related to the motor properties, ρ is the density of the surrounding air, A is the area swept out by the rotor, K_τ is a constant determined by the blade configuration and parameters, and b is the thrust factor.

The torque around the axis of rotor i, for $i = 1, \ldots, 4$, generated due to drag is given by

$$M_i = \frac{1}{2} R \rho C_D A (\omega_i R)^2 = d\omega_i^2 \tag{2-2}$$

where R is the radius of the propeller, C_D is a dimensionless constant, and d is the drag constant.

For given desired total thrust f and total moment $M = \begin{bmatrix} M_\phi & M_\theta & M_\psi \end{bmatrix}^T$, the required rotor speeds can be calculated by solving the following equation

$$
\begin{bmatrix} f \\ M_\phi \\ M_\theta \\ M_\psi \end{bmatrix} = \begin{bmatrix} b & b & b & b \\ 0 & -lb & 0 & lb \\ lb & 0 & -lb & 0 \\ -d & d & -d & d \end{bmatrix} \begin{bmatrix} \omega_1^2 \\ \omega_2^2 \\ \omega_3^2 \\ \omega_4^2 \end{bmatrix}
\tag{2-3}
$$

where l is the distance from the rotor to the QR's CoM and M_ϕ, M_θ, M_ψ denote the moments around the x, y, z-axis in $\{\mathcal{B}\}$, resp.

Table 2-1 shows the most common assumptions that are used for modeling the QR, simplifying the complexity of the model.

****

Bart: Refer to table 2-2?
Nam: Wat bedoel je?

****

Modeling assumptions Quadrotor model
• The structure of the QR is rigid and symmetric.   Elastic deformations and shock (sudden accelerations) of the QR are ignored.   • The mass distribution of the QR is symmetrical in the x-y plane.   • The inertia matrix is time-invariant.   • Aerodynamic effects acting on the QR are neglected.   Blade flapping, Turbulence, Ground Effects.   • The air density around the QR is constant.   • The propellers are rigid $\Rightarrow$ The thrust produced by rotor i is parallel to the axis of rotor i.   • Drag factor d and thrust factor b are approximated by a constant.   Thrust force F_i and moment M_i of each propeller is proportional to the square of   the propeller speed.
Modeling assumptions Quadrotor-Load model
• The cable is modeled as a rigid and massless cable.   • The cable is connected to a friction-less joint at the origin of the body-fixed.   • The tension in the cable is considered to be non-zero.   This implies that the QR-Load subsystem, consisting of a separate QR and Load   in free fall, is disregarded.   • Aerodynamic effects acting on the load are neglected.   reference frame.   • Assumption   Details Assumption 2

Table 2-1: Modeling assumptions

2-2   Geometric Mechanics

In Geometric Mechanics the configuration space of systems is a *group manifold* instead of a Euclidean space. The kinetic and potential energies are expressed in terms of this configuration space and their tangent spaces. It explores the geometric structure of a Lagrangian- or Hamiltonian system through the concepts of vector calculus, linear algebra, differential geometry, and non-linear control theory. Geometric mechanics provides fundamental insights into the nonlinear system mechanics and yields useful tools for dynamics and control theory.

Euler angles are kinematically singular since the transformation from their time rates of change to the angular velocity vector is not globally defined. Furthermore, when angular errors are large, the difference in Euler angles is no longer a good metric to define the orientation error. Local coordinates often require symbolic computational tools due to complexity of multi-body systems. Hence, the error is rather written as the required rotation to get from the current to a desired orientation. As a result, the equations of motion and the control systems can be developed on a configuration manifold in a coordinate-free, compact, unambiguous manner, while singularities of local parameterization are avoided.

To illustrate the difference in configuration spaces, an example is given of a 2-link arm, where the configuration can be expressed by 2 coordinates, see in Figure 2-3. Figure 2-3b represents the configuration space as a Cartesian space, where the same dots represent one of the many identical configurations. This shows that this representation suffers from singularities caused by multiple points in one representation being mapped onto a single point in another representation. Figure 2-3c shows the configuration space as a geometric shape called a *torus*, a manifold where every configuration is mapped uniquely.

| (a) | (b) | (c) |
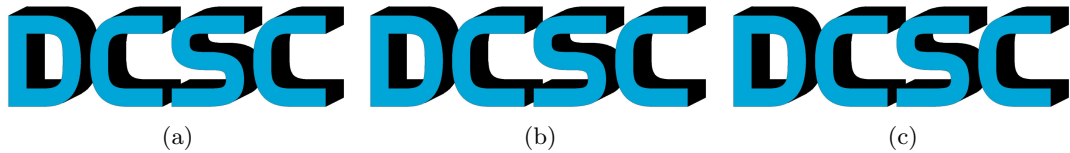
Figure 2-3: Configuration Space of a 2-link arm

Manifolds   The fundamental object of differential geometry a manifold. A manifold is a mathematical space, a collection of points, that locally resembles Euclidean space near each point. Examples are a plane, a ball, a torus and a sphere. Manifolds are important objects in mathematics and physics because they allow more complicated structures to be expressed and understood in terms of the relatively well-understood properties of simpler spaces. In Figure 2-4 is illustrated that each point of an n-dimensional manifold has a neighborhood that is homeomorphic to the n-dimensional Euclidean space, meaning that there is a continuous function describing the relation between these spaces.

A differentiable manifold is a smooth and continuous manifold and is locally similar enough to a linear space to allow to do calculus. One can define directions, tangent spaces, and differentiable functions on such a manifold. Each point of an n-dimensional differentiable manifold has a tangent space, which is an n-dimensional Euclidean space consisting of the

Figure 2-4: A manifold locally resembles a Euclidean space

tangent vectors of the curves through that point. In Figure 2-5a the manifold $\mathbb{S}^2$ is represented as a sphere, with a tangent space at point x, denoted by $T_x\mathbb{S}^2$. Taking the derivative at a point on a manifold is equivalent to a tangent vector at that point. Meaning that derivatives are conceptually equivalent to an infinitesimally short tangent vector.

(a) Representation of a manifold with a tangent space

(b) Identity map of $SO(3)$ with Lie Algebra $\mathfrak{so}(3)$

Figure 2-5

Configuration Spaces   Rotation matrices are used to provide a global representation of the attitude of a rigid body, by mapping a representation of vectors expressed in $\{\mathcal{B}\}$ to a representation expressed in $\{\mathcal{I}\}$ [10, 11]. The configuration of the QR attitude is a rotation matrix R in the Special Orthogonal Group $SO(3)$ defined as

$$SO(3) \triangleq \left\{ R \in \mathbb{R}^{3\times3} | RR^T = I_{3\times3}, det(R) = 1 \right\} \qquad (2\text{-}4)$$

$SO(3)$ is the group of all rotations about the origin of a 3-D Euclidean space, which preserves the origin, Euclidean distance and orientation. Every rotation has a unique inverse rotation and the identity map satisfies the definition of a rotation. The elements of *Lie Algebra* $\mathfrak{so}(3)$, a property associated with $SO(3)$, are the elements of the tangent space of $SO(3)$ at the identity element, see Figure 2-5b. These elements define the relation between the rotation R and its derivative $\dot{R}$, such that

$$\dot{R} = R\hat{\Omega} \qquad (2\text{-}5)$$

$\mathfrak{so}(3)$ is defined as

$$\mathfrak{so}(3) \triangleq \left\{ U \in \mathbb{R}^{3\times3} | U^T = -U \right\} \qquad (2\text{-}6)$$

Where a mapping from the angular velocity vector $\Omega \in \mathbb{R}^3$ to $\hat{\Omega} \in \mathfrak{so}(3)$ is defined as [11]

$$\hat{\Omega} = \begin{bmatrix} 0 & -\Omega_3 & \Omega_2 \\ \Omega_3 & 0 & -\Omega_1 \\ -\Omega_2 & \Omega_1 & 0 \end{bmatrix} \qquad (2\text{-}7)$$

The hat map $\hat{\cdot} : \mathbb{R}^3 \to \mathfrak{so}(3)$ is an isomorphism between $\mathbb{R}^3$ and the set of 3×3 skew symmetric matrices.

The configuration space of the load is represented on a 2-sphere, defined as

$$\mathbb{S}^2 \triangleq \left\{ q \in \mathbb{R}^3 | q \cdot q = 1 \right\} \tag{2-8}$$

$$\dot{q} = \omega \times q \tag{2-9}$$

where ω is the angular velocity of the suspended load.

2-3 Quadrotor-Load Model

In this section the model dynamics of the QR-Load system are obtained by describing the dynamics on nonlinear manifolds, with the concepts of differential geometry.

The focus lies on the subsystem where the cable tension is considered to be non-zero.

The Quadrotor-Load model is shown in Figure 2-6, where the unit vector q gives the direction from the QR to the Load expressed in $\{\mathcal{B}\}$.

Figure 2-6: Quadrotor-Load model representation

The derived mathematical model is represented by a set of dynamic equations commonly used for rigid body displacements.

Considering the properties of the system, the QR is described as a rigid body with six degrees of freedom, driven by forces and moments. Which means that the motion of a rigid body can be described by a translation of the Center of Mass (CoM) and a rotation about the CoM.

Dynamics and optimal control problems for rigid bodies are studied in [3], incorporating their geometric features. The focus lies on obtaining geometric properties of the dynamics of rigid bodies, how their configuration can be described and how these geometric properties are utilized in control system analysis and design.

The configuration of the QR can be described by the location of its CoM and its attitude, described in Euclidean space $x_Q \in \mathbb{R}^3$ and in a nonlinear space $R \in SO(3)$ respectively. Whereas the configuration of the load can also be described by its location and attitude, described in Euclidean space $x_L \in \mathbb{R}^3$ and on a two-sphere $q \in \mathbb{S}^2$.

The position of the QR and Load are related by

$$x_Q = x_L - Lq \tag{2-10}$$

where L is the length of the cable.

The attitude kinematics equation is given by

$$\dot{R} = R\hat{\Omega} \tag{2-11}$$

where $\Omega \in \mathbb{R}^3$ is the angular velocity represented in the body fixed frame, defined in Equation 2-7.

Variations on manifolds Looking at the variations on manifolds
This is different from traditional mechanics

To develop the Euler-Lagrange equations for mechanical systems that evolve on a Lie group, an approach developed by [3, 12, 13, 14] is used, which is based on Hamilton's principle.

The action integral is defined as

$$S = \int_{t_1}^{t_2} \mathcal{L} dt \tag{2-12}$$

where $\mathcal{L} = \mathcal{T} - \mathcal{U}$ is the Lagrangian of the system, where $\mathcal{T}, \mathcal{U}$ are the kinetic and potential energy, respectively. Hamilton's principle of least action states that the path a conservative mechanical system takes between two configurations at time t_1 and t_2, is the one for which Equation 2-12 is an extremum, stated as

$$\delta S = \int_{t_1}^{t_2} \delta \mathcal{L} dt = 0 \tag{2-13}$$

where $\delta \mathcal{L}$ is the variation of the Lagrangian. For systems with non-conservative forces and moments, Equation 2-13 is extended to

$$\delta S = \int_{t_1}^{t_2} (\delta W + \delta \mathcal{L}) dt = 0 \tag{2-14}$$

where δW is the virtual work. Equation 2-14 is applied to the QR-Load system, where the configuration manifold is $\mathbb{R}^3 \times \mathbb{S}^2 \times SO(3)$. With the following states

$$\mathbf{x} = \begin{bmatrix} x_L & \dot{x}_L & q & \omega & R & \Omega \end{bmatrix}^T \tag{2-15}$$

****

****
Rigid Body Attitude Dynamics evolve on $SE(3)$.

$$J\dot{\Omega} + \Omega \times J\Omega = mg\rho \times R^T e_3 + u \tag{2-16}$$

$$\dot{R} = R\hat{\Omega} \tag{2-17}$$

****

****
The equations of motion for a rigid body with configuration $SE(3)$ are given by the *Newton-Euler equations* [11]:

$$\begin{bmatrix} mI & 0 \\ 0 & \mathcal{I} \end{bmatrix} \begin{bmatrix} \dot{v}^b \\ \dot{\omega}^b \end{bmatrix} + \begin{bmatrix} \omega^b \times mv^b \\ \omega^b \times \mathcal{I}\omega^b \end{bmatrix} = F^b \tag{2-18}$$

where m is the mass of the body, $\mathcal{I}$ is the inertia tensor, and $V^b = (v^b, \omega^b)$ and F^b represent the instantaneous body velocity and applied body wrench.
****

****
The load dynamics evolve on $\mathbb{S}^2$. Based on [14].
****

2-4 Classical Modeling

This section describes the derivation of the model by using classical modeling techniques.
****
Reference **??**
****

When assuming small angle maneuvers, *Euler-angles* can be used to locally parameterize the orientation of the body-fixed reference coordinate frame with respect to the inertial reference coordinate frame. Simple linear controllers are often based on a linearized dynamical model, applying this small angles assumption.

From Newton's law follows

$$
\begin{aligned}
\dot{x}_Q &= v_Q \\
m_Q \dot{v}_Q &= fRe_3 - m_Q ge_3 - Tq \\
\dot{x}_L &= v_L \\
m_L \dot{v}_L &= -m_L ge_3 + Tq
\end{aligned}
\tag{2-19}
$$

Because the Euler-Angles are used, a function is required that maps a vector of the Z-X-Y Euler angles to its rotation matrix $R \in SO(3)$, which is denoted as [15]

$$
R_{312}(\phi, \theta, \psi) = \begin{bmatrix} c_\psi c_\theta - s_\phi s_\psi s_\theta & -c_\phi s_\psi & c_\psi s_\theta + c_\theta s_\phi s_\psi \\ c_\theta s_\psi + c_\psi s_\phi s_\theta & c_\phi c_\psi & s_\psi s_\theta - c_\psi c_\theta s_\phi \\ -c_\phi s_\theta & s_\phi & c_\phi c_\theta \end{bmatrix}
\tag{2-20}
$$

The Z-X-Y Euler angles to model the rotation can be seen in Figure 2-7. The first rotation by yaw angle ψ is around the z-axis of $\{\mathcal{I}\}$. Next is the rotation by roll angle ϕ, and the last rotation is by pitch angle θ.

The unit vector q from the QR to the load is represented in $\{\mathcal{B}\}$. Define ϕ_L as the yaw-rotation of the load around the z-axis of $\{\mathcal{B}\}$ and θ_L as the angle between the cable and the z-axis of $\{\mathcal{B}\}$, see Figure 2-8.

$$
q = \begin{bmatrix} s_{\theta_L} c_{\phi_L} \\ s_{\theta_L} s_{\phi_L} \\ c_{\theta_L} \end{bmatrix}
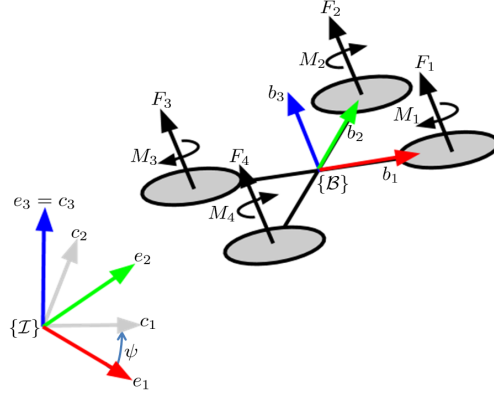\tag{2-21}
$$

Figure 2-7: Quadrotor-Load model representation

Figure 2-8

Differentiating Equation (2-10) and (2-21) gives

$$\ddot{x}_L = \ddot{x}_Q - \ddot{q}L$$

$$\ddot{q} = \begin{bmatrix} \ddot{\theta}_L c_{\theta_L} c_{\phi_L} - \ddot{\phi}_L s_{\theta_L} s_{\phi_L} - \dot{\phi}_L^2 s_{\theta_L} c_{\phi_L} - \dot{\theta}_L^2 s_{\theta_L} c_{\phi_L} - 2\dot{\theta}_L \dot{\phi}_L c_{\theta_L} s_{\phi_L} \\ \ddot{\theta}_L c_{\theta_L} s_{\phi_L} + \ddot{\phi}_L s_{\theta_L} c_{\phi_L} - \dot{\phi}_L^2 s_{\theta_L} s_{\phi_L} - \dot{\theta}_L^2 s_{\theta_L} s_{\phi_L} + 2\dot{\theta}_L \dot{\phi}_L c_{\theta_L} c_{\phi_L} \\ -\ddot{\theta}_L s_{\theta_L} - \dot{\theta}_L^2 c_{\theta_L} \end{bmatrix} \quad (2\text{-}22)$$

$$\ddot{x}_Q = \frac{1}{m_Q}(f(c_\psi s_\theta + c_\theta s_\phi s_\psi) - T s_{\theta_L} c_{\psi_L})$$

$$\ddot{y}_Q = \frac{1}{m_Q}(f(s_\psi s_\theta - c_\psi c_\theta s_\phi) - T s_{\theta_L} s_{\psi_L}) \quad (2\text{-}23)$$

$$\ddot{z}_Q = \frac{1}{m_Q}(f(c_\phi c_\theta) - T c_{\theta_L}) - g$$

$$\ddot{\psi} = \tilde{\tau}_\psi \quad (2\text{-}24)$$

$$\ddot{\theta} = \tilde{\tau}_\theta \quad (2\text{-}25)$$

$$\ddot{\phi} = \tilde{\tau}_\phi \quad (2\text{-}26)$$

2-5 Stability Analysis

Lyapunov Analysis on SO3 x R3 and S2 x R3 Closed-loop full-attitude dynamics evolve on the non- Euclidean manifold SO3 x R3, while closed-loop re- duced-attitude dynamics evolve

on the non-Euclidean mani- fold S2 x R3. Since these manifolds are locally Euclidean, local stability properties of a closed-loop equilibrium solution can be assessed using standard Lyapunov methods. In ad- dition, the LaSalle invariance result and related Lyapunov results apply to closed-loop vector fields defined on these manifolds. However, since the manifolds SO132 and S2 are compact, the radial unboundedness assumption cannot be satisfied; consequently, global asymptotic stability cannot fol- low from a Lyapunov analysis on Euclidean spaces [40], and therefore must be analyzed in alternative ways [19]–[23].[10, p.43]

2-6   Summary

****

Compact, unambiguous, globally defined,

Pro/Cons of Classical Modeling Techniques vs Geometric Modeling

Linearized model/State Space model vs. Geometric modeling

Geometric Mechanics/Lie Groups/Lie Algebra is used in order to represent the dynamics of the system onto the nonlinear configuration manifold $SE(3)$
Advantage of this method is
Enables to model on
That type of control is discussed in the next chapter

****

Chapter 3

Geometric Control Design

[8, 9]

Geometric Control Theory explores the application of differential geometric techniques to systems control. The objective is to express both the dynamics and its control inputs on manifolds instead of on local charts. Geometric control theory is the study of how the geometry of the state space influences controls problems. This includes local properties like curvature, and global properties like the number of 'holes' in the space (sphere vs doughnut).

Geometric Control is based on a coordinate-free representation of the dynamics, where the equations of motion are compact, unambiguous and singularity free. Globally defined (no singularities!). Therefore, one can build almost globally attractive controllers

Attitude control systems naturally evolve on non-linear configurations such as $\mathbb{S}^2$ and $SO(3)$. Tracking control system can be developed on $SO(3)$, therefore it avoids singularities of Euler-Angles.

Global nonlinear dynamics of various classes of closed loop attitude control systems have been studied in recent years [?]. In contrast to hybrid control systems [16], **complicated reachability set analysis is not required** to guarantee safe switching between different flight modes, as the region of attraction for each flight mode covers the configuration space almost globally.

3-1 Backstepping Control

A backstepping approach, or cascade control, is a Lyapunov based technique to design the control of nonlinear dynamical systems, while ensuring Lyapunov stability. The principle is to create a cascaded structure by starting with a stable system as a base, then "stepping back" from the base to add a control loop around it that stabilizes the added subsystem. This is repeated until the the final external control is reached. The control law is designed by using states as virtual control signals. Each loop outputs a virtual command signal, denoted by subscript c, for the inner loop to track in order to control the outer loop.

Figure 3-1: Backstepping Control representation of the QR

A backstepping control approach is common for QRs [**?**] and can be seen in Figure 3-1. The lowest level has the highest bandwidth and is in control of the rotor rotational speeds. The next level controls the QR attitude, and the top level controls the QR position.

Because the QR has only four actuators, it is not possible to control all DOFs of the QR-Load system. Therefore, different flight modes are specified in which parts of the DOFs are controlled. The same backstepping approach allows different flight modes that are defined as follows

- QR Attitude Controlled Mode
    - Track a desired QR attitude command $R_d(t)$ and a heading direction $b_{1_d}(t)$
- Load Attitude Controlled Mode
    - Track a desired load attitude command $q_d(t)$
- Load Position Controlled Mode
    - Track a desired load position $x_{L,d}(t)$

Figure 3-2: Backstepping Control representation of the QR-Load system

3-2 Configuration Errors

****

Most of nonlinear dynamics and control problems are studied in a linear space.

$$\dot{x} = \mathbf{f}(t, x, u), \quad x \in \mathbb{R}^n, u \in \mathbb{R}^m, \mathbf{f} : \mathbb{R}^{n+m+1} \to \mathbb{R}^n \qquad (3\text{-}1)$$

In control systems engineering, the underlying geometric features of a dynamic system are often not considered carefully. For example, many control systems are developed for the standard form of ordinary differential equations, namely $\dot{x} = f(x, u)$, where the state and the control input are denoted by x and u. It is assumed that the state and the control input lie in

Euclidean spaces, and the system equations are defined in terms of smooth functions between Euclidean spaces. However, for many interesting mechanical systems, the configuration space cannot be expressed globally as a Euclidean space.

****

Before the controllers are described, the configuration functions are defined as in [8]. These functions describe the error on the manifolds $SO(3)$ and $\mathbb{S}^2$, which describe the configuration spaces for the QR attitude and the load attitude, respectively.

Define errors associated with the attitude dynamics of the QR. The attitude and angular velocity tracking error should be carefully chosen as they evolve on the tangent bundle of $SO(3)$. [?]

The error function on $SO(3)$ is chosen to be [17]

$$\Psi_R(R, R_d) = \frac{1}{2} tr\left[I - R_d^T R\right] \tag{3-2}$$

The error function on $\mathbb{S}^2$ is chosen to be

$$\Psi_q \tag{3-3}$$

The tracking error functions on the tangent space of $SO(3)$, denoted by $TSO(3)$ are defined as

$$e_R \tag{3-4}$$

$$e_\Omega \tag{3-5}$$

The tracking error functions on the tangent space of $\mathbb{S}^2$, denoted by $T\mathbb{S}^2$ are defined as

$$e_q \tag{3-6}$$

$$e_{\dot{q}} \tag{3-7}$$

The tracking errors for position and velocity are defined as

$$e_x = x - x_d \tag{3-8}$$
$$e_v = v - v_d \tag{3-9}$$
$$\text{where, } v_d = \dot{x}_d \tag{3-10}$$

where $x_d(t) \in \mathbb{R}^3$ is a smooth desired load position.

Figure 3-3

3-3 Quadrotor Attitude Tracking

This control problem has been addressed in various works *****

The most inner loop controls the attitude of the QR.

Attitude control problem is the inner loop of the control design. This inner loop must guarantee stability of the QR.

Must track reference attitude.

The attitude and angular velocity tracking error should be carefully chosen as the evolve on the tangent bundle of the nonlinear space $SO(3)$. [17]
Why? Appendix[17], and [8]?

The moment consists of a proportional term, a derivative term and a canceling term, and is defined as follows

$$M = \frac{1}{\epsilon^2}k_R eR - \frac{1}{\epsilon}k_\Omega e_\Omega + \Omega \times J_Q\Omega - J_Q(\hat{\Omega}R^T R_d\Omega_d - R^T R_d\dot{\Omega}_d) \tag{3-11}$$

****

Asymptotic tracking of the quadrotor attitude does not require specification of the thrust magnitude. As an auxiliary problem, the thrust magnitude can be chosen in many different ways to achieve an additional translational motion objective. For example, it can be used to asymptotically track a quadrotor altitude command [28]. Since the translational motion of the quadrotor UAV can only be partially controlled; this flight mode is most suitable for short time periods where an attitude maneuver is to be completed. [19]

****

Control input [14]
$$u = -k_R e_R - k_\Omega \Omega - mg\rho \times R^T e_3 \tag{3-12}$$

Insert into Equation 2-16; closed loop dynamics are given by

$$J\dot{\Omega} = -\Omega \times J\Omega - k_R e_R - k_\Omega \Omega \tag{3-13}$$

$$\dot{R} = R\hat{\Omega} \tag{3-14}$$

3-4 Load Attitude Tracking

Tracks load attitude reference. Outputs attitude reference to attitude controller.

Figure 3-4

How is the controller built.

Dependent of what values? How to choose parameters.

$$R = \tag{3-15}$$

3-5   Load Position Tracking

Tracks load position reference. Outputs load attitude reference.

$$q = \tag{3-16}$$

Figure 3-5

3-6   Parameter- and State Estimation

How to choose parameters and how to select gains for errors

How to estimate states?

What parameters must be

Refer to Lyapunov stability analysis [8]

3-7   Summary

****
What is Geometric Control?
Why Geometric Control?

Control design will be based on Nonlinear Geometric Control

The proposed control system is robust to switching conditions since each flight mode has almost global stability properties, and it is straightforward to design a complex maneuver of a QR. [20] Where are the Error functions based on?

Form bridge between Geometric Control and Hybrid Control
Why Hybrid Control?
Parameter Estimation can be done by

State Estimation can be done by

Drawback: assumes all states to be known

Model based. What if analytical model is not accurate?
****

Chapter 4

Experiments and Results

4-1 Setup

Model parameters The simulations are developed using Matlab and Simulink, using the following system parameters.

$$J = \qquad d = \qquad m_L =$$
$$m_Q = \qquad c_{\tau f} = \qquad l_L =$$

LQR Control LQR control is based on small angle assumption. Therefore, a traditional modeling method may represent the rotation matrix with a local coordinate system, for example with a Euler Angle parameterization. An LQR control design is based on a linearized model of the system. The control design is shown in Figure 4-1 and the derivation of the model can be found in Section A-2.

Figure 4-1: LQR control design

The tuning parameters of the LQR controller a chosen as follows

$$A = \begin{bmatrix} content... \end{bmatrix} \tag{4-1}$$

$$B = \begin{bmatrix} content... \end{bmatrix} \tag{4-2}$$

$$C = \begin{bmatrix} content... \end{bmatrix} \tag{4-3}$$

where the state $\mathbf{x}$ and input u are defined as

$$\mathbf{x} = \begin{bmatrix} \mathbf{q} \\ \dot{\mathbf{q}} \end{bmatrix} \tag{4-4}$$

$$\mathbf{q} = \begin{bmatrix} x & y & z & \phi & \theta & \psi & \theta_L & \psi_L \end{bmatrix}^T \tag{4-5}$$

$$\dot{\mathbf{q}} = \begin{bmatrix} \dot{x} & \dot{y} & \dot{z} & \dot{\phi} & \dot{\theta} & \dot{\psi} & \dot{\theta}_L & \dot{\psi}_L \end{bmatrix}^T \tag{4-6}$$

$$u = \begin{bmatrix} f & M_\phi & M_\theta & M_\psi \end{bmatrix}^T \tag{4-7}$$

Geometric Control   The controller gains in Equations 3-11,3-15,3-16 are chosen to be

$$k_R = \qquad k_q = \qquad k_x =$$
$$k_\Omega = \qquad k_\omega = \qquad k_v =$$

4-1-1   Command Filtering

Implementation of the backstepping approach also increases the order of the states. Thus, a consequence of backstepping control is that inner control loops become a function of the commanded signals and their higher derivatives, generated by an outer loop. Instead of analytic differentiation of these terms, which can be tedious and require high computational costs, these values can be obtained with the use of a Command Filter, which is explained in more detail in [21].

Basically, the command signal is pre-filtered by a low pass filter

with the following state space representation

$$\dot{x}_1 = x_2 \tag{4-8}$$

$$\dot{x}_2 = x_3 \tag{4-9}$$

$$\dot{x}_3 = -(2\zeta\omega_{n2} + \omega_{n1})x_3 - (2\zeta\omega_{n1}\omega_{n2} + \omega_{n2}^2)x_2 - (\omega_{n1}\omega_{n2}^2)(x_1 - x_c^o) \tag{4-10}$$

where $x_1 = x_c$, $x_2 = \dot{x}_c$ and $x_3 = \ddot{x}_c$.

The transfer function of the original commanded input signal X_c^o and the filtered output X_c has the form

$$\frac{X_c(s)}{X_c^o(s)} = H(s) = \frac{\omega_{n1}}{s + \omega_{n1}} \cdot \frac{\omega_{n2}^2}{s^2 + 2\zeta\omega_{n2}s + \omega_{n2}^2} \tag{4-11}$$

Where ζ is the damping ratio and ω_n the undamped natural frequency. See Figure 4-2 and A-1.

This command filter is implemented to compute $\dot{R}_c, \ddot{R}_c, \dot{q}_c, \ddot{q}_c$.

****

Easy implementation. Less computational effort.

Less accurate, because filters high frequency signals.

****

The load attitude controller generates a commanded QR attitude R_c and its derivative $\dot{R}_c$. In the same fashion, the load position controller generates a commanded load attitude q_c and its derivative $\dot{q}_c$.

The controllers are functions of these commanded signals and their derivatives. Instead of analytic differentiation of these signals, they are obtained by integration by applying a third order low pass filter to the original signals R_c^o and q_c^o. The state space implementation of this third order filter is [22]

Figure 4-2: Representation of the command filter

$$\frac{x_c}{x_c^o} = \frac{\omega_{n1}}{s + \omega_{n1}} \cdot \frac{\omega_{n2}^2}{s^2 + 2\zeta\omega_{n2}s + \omega_{n2}^2} \tag{4-12}$$

$$\Rightarrow x_c''' = -(2\zeta\omega_{n2} + \omega_{n1})x_c'' - (2\zeta\omega_{n1}\omega_{n2} + \omega_{n2}^2)x_c' - (\omega_{n1}\omega_{n2}^2)(x_c - x_c^o) \tag{4-13}$$

4-2 Experiments

LQR is an optimal control strategy and will be used to compare its result to a Nonlinear Geometric Controller.

4-2-1 Performance Criteria

Performance that can be evaluated for different cases can be specified as the following items.

- Step Response
  - Settling time (if swing minimization is important)
  - Rising time (important if time critical)
  - Overshoot (if max swing is critical)
  - Steady state error / swing of load (if accuracy is important)
  - Max load angle

- Disturbance Rejection

- Trajectory tracking
  - Can we minimize time, while minimizing position error (All Cases)

  – Minimum position error (All Cases)

  – Maximum amplitude/frequency of wave with respect to stability (Case B)

• Computational Effort (?)

Explain cases, why interesting and what can be expected?

4-2-2   Case A

4-2-3   Case B

4-2-4   Case C

Figure 4-3: Cases of which the performance could be evaluated

4-3   Results

4-3-1   Case A

4-3-2   Case B

4-3-3   Case C

4-4   Conclusion

Chapter 5

Conclusions and Future Work

5-1   Summary and Conclusions

The report starts with an introduction to the subject. The aim is described and the motivation for this research is given.

In the following chapter A short introduction of the concepts of differential geometry

Next, the nonlinear geometric control design is explained. Backstepping is explained

Experiments are defined. Testing the nonlinear Geometric Controller To compare with a common linear controller, LQR control is used to compare Results are,

The conclusions we could extract from the experiments is that

5-2   Recommendations for Future Work

5-2-1   Investigate Implementation

Lack of time: no implementation possible. In order to realize this, one needs to investigate the subjects described in this section.

Can in be implemented in terms of computational power? Can this be run on on-board processor? Problem is already partly simplified by command filter. Quantification and comparison between implemented MPC and Geometric Control.

Model identification and validation. Now it is an estimation and/or taken from other literature.

5-2-2   Modeling Constraints

There are several techniques to handle input saturation, the most popular ones are anti-windup techniques. Back-calculation is such a method for PID to activate the integrator, is this possible for NL control?

****

[4] includes uncertainties in the translational dynamics and rotational dynamics. Out of the scope, might be interesting.
****

5-2-3   Hybrid Modeling

Switching between several flight modes yields autonomous acrobatic maneuvers. Robust to switching conditions ***why?
[23]

5-2-4   Trajectory Generation

Minimum Snap Trajectory Generation

Trajectory can be generated by solving a **QP!** via minimum snap generation.

Problem in smaller 4-D space instead of 12-D, with help of differential flatness. Explain differential flatness and its usefulness.

Is able to include constraints in **QP!**.

[18]

Obstacle avoidance

Appendix

A-1 Derivation of Equations of motion

A-1-1 Load Dynamics

Let x_{CM} denote the position of the center of mass of the combined Quadrotor-Load system, expressed in $\{\mathcal{I}\}$. Which can be found by

$$
\begin{aligned}
m_Q(x_Q - x_{CM}) + m_L(x_L - x_{CM}) &= 0 \\
(m_Q + m_L)x_{CM} &= m_Q x_Q + m_L x_L
\end{aligned}
\tag{A-1}
$$

Applying the laws of motion to (A-1) and inserting (2-10) gives the

$$
\begin{aligned}
(m_Q + m_L)\ddot{x}_{CM} &= fRe_3 - (m_Q + m_L)ge_3 \\
(m_Q + m_L)(\ddot{x}_L + ge_3) &= fRe_3 + m_Q L\ddot{q}
\end{aligned}
\tag{A-2}
$$

A-2 Derivation of LQR controller

A-2-1 Modeling

From Newton's laws follows

$$
x_Q = fRe_3 - m_Q ge_3 - Tq
\tag{A-3}
$$

$$
x_L = -m_L ge_3 + Tq
\tag{A-4}
$$

x_Q and x_L are related by

$$
x_L = x_Q + Lq
\tag{A-5}
$$

$$\ddot{x} =$$
$$\ddot{y} = \tag{A-6}$$
$$\ddot{z} =$$

$$\ddot{\phi} =$$
$$\ddot{\theta} = \tag{A-7}$$
$$\ddot{\psi} =$$

$$\ddot{\phi}_L =$$
$$\ddot{\theta}_L = \tag{A-8}$$

A-2-2 Controller

$$\mathbf{x} = \begin{bmatrix} \mathbf{q} \\ \dot{\mathbf{q}} \end{bmatrix} \tag{A-9}$$

$$\mathbf{q} = \begin{bmatrix} x & y & z & \phi & \theta & \psi & \theta_L & \psi_L \end{bmatrix}^T \tag{A-10}$$

$$\dot{\mathbf{q}} = \begin{bmatrix} \dot{x} & \dot{y} & \dot{z} & \dot{\phi} & \dot{\theta} & \dot{\psi} & \dot{\theta}_L & \dot{\psi}_L \end{bmatrix}^T \tag{A-11}$$

$$u = \begin{bmatrix} f & M_\phi & M_\theta & M_\psi \end{bmatrix}^T \tag{A-12}$$

$$\dot{\mathbf{x}} = A\mathbf{x} + Bu \tag{A-13}$$
$$y = C\mathbf{x} + Du \tag{A-14}$$

$$\dot{\mathbf{x}} = \mathbf{f}(\mathbf{x}, \mathbf{u}) \tag{A-15}$$

By linearizing Equations A-6,A-7,A-8 follows

$$\ddot{x} = -\frac{f}{m} \tag{A-16}$$

$$\ddot{y} = \tag{A-17}$$

$$\ddot{z} = \tag{A-18}$$

The mathematical model is linearized around the following operating points

$$\bar{\mathbf{x}} = \begin{bmatrix} \bar{x} & \bar{y} & \bar{z} & \mathbf{0}_{1 \times 13} \end{bmatrix}^T \tag{A-19}$$

$$\bar{\mathbf{u}} = \begin{bmatrix} (m_Q + m_L)g & 0 & 0 & 0 \end{bmatrix}^T \tag{A-20}$$

Assuming small angles, the following holds

$$\text{for } \gamma = \phi, \theta, \psi, \theta_L, \psi_L \tag{A-21}$$

$$sin(\gamma) \simeq \gamma \tag{A-22}$$

$$cos(\gamma) \simeq 1 \tag{A-23}$$

$$\dot{\gamma} \simeq 0 \tag{A-24}$$

$$F \simeq (m_Q + m_L)g \tag{A-25}$$

$$A = \frac{\partial \mathbf{f}(x, u)}{\partial x} \Big|_{x=\bar{x}, u=\bar{u}} \tag{A-26}$$

$$B = \frac{\partial \mathbf{f}(x, u)}{\partial u} \Big|_{x=\bar{x}, u=\bar{u}} \tag{A-27}$$

$$u = -K \left[\mathbf{x}_{des}(t) - \mathbf{x}(t) \right] \tag{A-28}$$

A-3   Figures

Figure A-1: Simulink Command Filter

A-4   `MATLAB` **code**

$$Testequation \tag{A-29}$$

A-4-1   A MatlabListing

```
%                                                                          1
% Comment
%
n=10;
for i=1:n
    disp('Ok');                                                           6
end
```

Bibliography

[1] M. Bangura and R. Mahony, "Real-time model predictive control for quadrotors," in *IFAC Proceedings Volumes (IFAC-PapersOnline)*, vol. 19, pp. 11773–11780, 2014.

[2] R. P. K. Jain and T. Keviczky, "MSc Thesis: Transportation of Cable Suspended Load using Unmanned Aerial Vehicles: A Real-time Model Predictive Control approach," 2015.

[3] T. Lee, *Computational Geometric Mechanics and Control of Rigid Bodies*. PhD thesis, The University of Michigan, 2008.

[4] F. Goodarzi, D. Lee, and T. Lee, "Geometric nonlinear PID control of a quadrotor UAV on SE (3)," *Control Conference (ECC), 2013 European*, pp. 3845–3850, 2013.

[5] K. Sreenath, T. Lee, and V. Kumar, "Geometric control and differential flatness of a quadrotor UAV with a cable-suspended load," in *Proceedings of the IEEE Conference on Decision and Control*, pp. 2269–2274, 2013.

[6] S. Tang and V. Kumar, "Mixed Integer Quadratic Program Trajectory Generation for a Quadrotor with a Cable-Suspended Payload," *IEEE International Conference on Robotics and Automation (ICRA)*, pp. 2216–2222, 2015.

[7] W. M. Boothby, *An Introduction to Differentiable Manifolds and Riemannian Geometry*. 2003.

[8] F. Bullo and A. D. Lewis, *Geometric control of mechanical systems: modeling, analysis, and design for simple mechanical control systems*. Springer, 2005.

[9] V. Jurdjevic, *Geometric Control Theory*. Cambridge: Cambridge University Press, 1997.

[10] N. Chaturvedi, A. Sanyal, and N. McClamroch, "Rigid-Body Attitude Control," *IEEE Control Systems*, vol. 31, no. 3, pp. 30–51, 2011.

[11] R. M. Murray, Z. Li, and S. S. Sastry, *A Mathematical Introduction to Robotic Manipulation*, vol. 29. 1994.

[12] T. L. T. Lee, N. McClamroch, and M. Leok, "A lie group variational integrator for the attitude dynamics of a rigid body with applications to the 3D pendulum," *Proceedings of 2005 IEEE Conference on Control Applications, 2005. CCA 2005.*, pp. 962–967, 2005.

[13] T. Lee, M. Leok, and N. H. McClamroch, "Lagrangian mechanics and variational integrators on two-spheres," *International Journal for Numerical Methods in Engineering*, vol. 79, no. 9, pp. 1147–1174, 2009.

[14] T. Lee, M. Leok, and N. H. McClamroch, "Stable Manifolds of Saddle Points for Pendulum Dynamics on S^2 and SO(3)," p. 9, 2011.

[15] R. Mahony, V. Kumar, and P. Corke, "Multirotor Aerial Vehicles: Modeling, Estimation, and Control of Quadrotor," *IEEE Robotics & Automation Magazine*, vol. 19, no. 3, pp. 20–32, 2012.

[16] J. H. Gillula, H. Huang, M. P. Vitus, and C. J. Tomlin, "Design of guaranteed safe maneuvers using reachable sets: Autonomous quadrotor aerobatics in theory and practice," in *Proceedings - IEEE International Conference on Robotics and Automation*, pp. 1649–1654, 2010.

[17] T. Lee, M. Leok, and N. H. Mcclamroch, "Geometric Tracking Control of a Quadrotor UAV on SE(3)," *49th IEEE Conference on Decision and Control*, no. 3, pp. 5420–5425, 2010.

[18] D. Mellinger and V. Kumar, "Minimum snap trajectory generation and control for quadrotors," in *Proceedings - IEEE International Conference on Robotics and Automation*, pp. 2520–2525, 2011.

[19] F. A. Goodarzi, "Geometric Nonlinear Controls for Multiple Cooperative Quadrotor UAVs Transporting a Rigid Body," no. December 2009, 2015.

[20] T. Lee, M. Leok, and N. McClamroch, "Control of complex maneuvers for a quadrotor UAV using geometric methods on SE (3)," *arXiv*, 2010.

[21] J. A. Farrell, M. Polycarpou, M. Sharma, and W. Dong, "Command Filtered Backstepping," pp. 1923–1928, 2008.

[22] V. Djapic, J. Farrell, and W. Dong, "Land vehicle control using a command filtered backstepping approach," *Proceedings of the American Control Conference*, pp. 2461–2466, 2008.

[23] S. Tang, "Aggressive Maneuvering of a Quadrotor with a Cable-Suspended Payload," tech. rep., University of Pennsylvania Philadelphia, Pennsylvania, 2014.

Bibliography

[1] M. Bangura and R. Mahony, "Real-time model predictive control for quadrotors," in *IFAC Proceedings Volumes (IFAC-PapersOnline)*, vol. 19, pp. 11773–11780, 2014.

[2] R. P. K. Jain and T. Keviczky, "MSc Thesis: Transportation of Cable Suspended Load using Unmanned Aerial Vehicles: A Real-time Model Predictive Control approach," 2015.

[3] T. Lee, *Computational Geometric Mechanics and Control of Rigid Bodies*. PhD thesis, The University of Michigan, 2008.

[4] F. Goodarzi, D. Lee, and T. Lee, "Geometric nonlinear PID control of a quadrotor UAV on SE (3)," *Control Conference (ECC), 2013 European*, pp. 3845–3850, 2013.

[5] K. Sreenath, T. Lee, and V. Kumar, "Geometric control and differential flatness of a quadrotor UAV with a cable-suspended load," in *Proceedings of the IEEE Conference on Decision and Control*, pp. 2269–2274, 2013.

[6] S. Tang and V. Kumar, "Mixed Integer Quadratic Program Trajectory Generation for a Quadrotor with a Cable-Suspended Payload," *IEEE International Conference on Robotics and Automation (ICRA)*, pp. 2216–2222, 2015.

[7] W. M. Boothby, *An Introduction to Differentiable Manifolds and Riemannian Geometry*. 2003.

[8] F. Bullo and A. D. Lewis, *Geometric control of mechanical systems: modeling, analysis, and design for simple mechanical control systems*. Springer, 2005.

[9] V. Jurdjevic, *Geometric Control Theory*. Cambridge: Cambridge University Press, 1997.

[10] N. Chaturvedi, A. Sanyal, and N. McClamroch, "Rigid-Body Attitude Control," *IEEE Control Systems*, vol. 31, no. 3, pp. 30–51, 2011.

[11] R. M. Murray, Z. Li, and S. S. Sastry, *A Mathematical Introduction to Robotic Manipulation*, vol. 29. 1994.

[12] T. L. T. Lee, N. McClamroch, and M. Leok, "A lie group variational integrator for the attitude dynamics of a rigid body with applications to the 3D pendulum," *Proceedings of 2005 IEEE Conference on Control Applications, 2005. CCA 2005.*, pp. 962–967, 2005.

[13] T. Lee, M. Leok, and N. H. McClamroch, "Lagrangian mechanics and variational integrators on two-spheres," *International Journal for Numerical Methods in Engineering*, vol. 79, no. 9, pp. 1147–1174, 2009.

[14] T. Lee, M. Leok, and N. H. McClamroch, "Stable Manifolds of Saddle Points for Pendulum Dynamics on Sˆ2 and SO(3)," p. 9, 2011.

[15] R. Mahony, V. Kumar, and P. Corke, "Multirotor Aerial Vehicles: Modeling, Estimation, and Control of Quadrotor," *IEEE Robotics & Automation Magazine*, vol. 19, no. 3, pp. 20–32, 2012.

[16] J. H. Gillula, H. Huang, M. P. Vitus, and C. J. Tomlin, "Design of guaranteed safe maneuvers using reachable sets: Autonomous quadrotor aerobatics in theory and practice," in *Proceedings - IEEE International Conference on Robotics and Automation*, pp. 1649–1654, 2010.

[17] T. Lee, M. Leok, and N. H. Mcclamroch, "Geometric Tracking Control of a Quadrotor UAV on SE(3)," *49th IEEE Conference on Decision and Control*, no. 3, pp. 5420–5425, 2010.

[18] D. Mellinger and V. Kumar, "Minimum snap trajectory generation and control for quadrotors," in *Proceedings - IEEE International Conference on Robotics and Automation*, pp. 2520–2525, 2011.

[19] F. A. Goodarzi, "Geometric Nonlinear Controls for Multiple Cooperative Quadrotor UAVs Transporting a Rigid Body," no. December 2009, 2015.

[20] T. Lee, M. Leok, and N. McClamroch, "Control of complex maneuvers for a quadrotor UAV using geometric methods on SE (3)," *arXiv*, 2010.

[21] J. A. Farrell, M. Polycarpou, M. Sharma, and W. Dong, "Command Filtered Backstepping," pp. 1923–1928, 2008.

[22] V. Djapic, J. Farrell, and W. Dong, "Land vehicle control using a command filtered backstepping approach," *Proceedings of the American Control Conference*, pp. 2461–2466, 2008.

[23] S. Tang, "Aggressive Maneuvering of a Quadrotor with a Cable-Suspended Payload," tech. rep., University of Pennsylvania Philadelphia, Pennsylvania, 2014.

Nomenclature

ω_i Angular velocity of rotor i around its axis, $i = \{1, 2, 3, 4\}$

$\tau_{drag,i}$ Drag moment generated by each propellor

$\{\mathbf{b}_1, \mathbf{b}_2, \mathbf{b}_3\}$ Unit vectors along the axes of $\{\mathcal{B}\}$

$\{\mathbf{c}_1, \mathbf{c}_2, \mathbf{c}_3\}$ Unit vectors along the axes of $\{\mathcal{C}\}$

$\{\mathbf{e}_1, \mathbf{e}_2, \mathbf{e}_3\}$ Unit vectors along the axes of $\{\mathcal{I}\}$

$\{\mathcal{B}\}$ Body Frame

$\{\mathcal{C}\}$ Intermediary Frame

$\{\mathcal{I}\}$ Inertial World Frame

b Thrust factor

d Drag factor

L Length of the cable

q Unit vector from Quadrotor to Load

x_L Position of the of the Quadrotor CM

x_Q Position of the of the Quadrotor CM

x_{CM} Position CM of Quadrotor-Load system

Acronyms

QR   Quadrotor

UAV   Unmanned Aerial Vehicle

CoM   Center of Mass

DOF   Degree of Freedom

PID controller Proportional-Integral-Derivative Controller

MPC   Model Predictive Control

Nonlinear MPC Nonlinear Model Predictive Control

LQR   Linear Quadratic Regulator

QP   Quadratic Programming